Published in final edited form as:

Cancer Res. 2020 March 01; 80(5): 999–1010. doi:10.1158/0008-5472.CAN-19-2205.

Nudix hydrolase NUDT16 regulates 53BP1 protein by reversing 53BP1 ADP-ribosylation

Fan Zhang[1,†], **Lihong Lou**[1,†], **Bo Peng**[1], **Xiaotian Song**[1], **Ofer Reizes**[2], **Alexandru Almasan**[1], **Zihua Gong**[1,*]

[1]Department of Cancer Biology, Cleveland Clinic Lerner Research Institute, Cleveland, Ohio;

[2]Department of Cardiovascular & Metabolic Sciences, Cleveland Clinic Lerner Research Institute, Cleveland, Ohio;

Abstract

53BP1 controls two downstream sub-pathways, one mediated by PTIP and Artemis and the other by RIF1 and MAD2L2/Shieldin, to coordinate DNA repair pathway choices. However, the upstream regulator(s) of 53BP1 function in DNA repair remain unknown. We and others recently reported that TIRR associates with 53BP1 to stabilize it and prevents 53BP1 localization to DNA damage sites by blocking 53BP1 Tudor domain binding to H4K20me2 sites. Here, we report that the Nudix hydrolase NUDT16, a TIRR homolog, regulates 53BP1 stability. We identified a novel post-translational modification of 53BP1 by ADP-ribosylation that is targeted by a PAR-binding E3 ubiquitin ligase, RNF146, leading to 53BP1 polyubiquitination and degradation. In response to DNA damage, ADP-ribosylated 53BP1 increased significantly, resulting in its ubiquitination and degradation. These data suggest that NUDT16 plays a major role in controlling 53BP1 levels under both normal growth conditions and during DNA damage. Notably, overexpression of a NUDT16 catalytically inactive mutant blocked 53BP1 localization to double-strand breaks because: 1) the mutant binding to TIRR increased after IR; 2) the mutant enhanced 53BP1 Tudor domain binding to TIRR, and 3) the mutant impaired the interaction of 53BP1 Tudor domain with H4K20me2. Moreover, NUDT16's catalytic hydrolase activity was required for 53BP1 de-ADP-ribosylation, 53BP1 protein stability, and its function in cell survival. In summary, we demonstrate that NUDT16 regulates 53BP1 stability and 53BP1 recruitment at double-strand breaks, providing yet another mechanism of 53BP1 regulation.

INTRODUCTION

DNA double-strand breaks (DSBs) are the most consequential type of DNA damage because, if unrepaired, they lead to genetic instability and are implicated in many human diseases. Two distinct pathways are involved in the repair of DNA DSBs: non-homologous DNA end- joining (NHEJ), which rejoins the broken ends without the use of extensive

*Corresponding Author: Zihua Gong, Cleveland Clinic Lerner Research Institute, 9500 Euclid Avenue, Cleveland, OH44195. Phone: 216-445-9652. gongz@ccf.org.

†These authors contributed equally to this work.

Conflict of Interest:

The authors declare no potential conflicts of interest.

homology; and homologous recombination (HR), which requires a homology template from an undamaged sister chromatid chromosome. A deep understanding of DNA repair pathway choice not only is crucial to our understanding of cancer, but also provides new targets for cancer therapies.

The protein 53BP1 has attracted particular attention in DNA repair because of its role in the choice between NHEJ and HR and its relevance to PARP inhibitor (PARPi) treatment of BRCA1-mutant cancers. 53BP1 contains a highly phosphorylated N-terminal region, a Tudor domain in the middle, and two BRCT domains at its C-terminus. The formation of 53BP1 foci at DNA damage sites requires binding of H4K20me2 via its Tudor domain (1). In support of the roles that histone methylation plays in 53BP1 localization, one of the histone methyltransferases, MMSET, has been implicated in 53BP1 recruitment at sites of DNA damage (2). The IRIF (ionizing radiation-induced foci) region of 53BP1 also contains a ubiquitination-dependent recruitment motif. Recent studies suggest that accumulation of 53BP1 at DNA damage sites requires both domains plus histone ubiquitination at H2AX K13/K15 sites (3), which is mediated by RNF8/RNF168 in the H2AX-dependent pathway (4–9).

53BP1 is generally hypothesized to be an adaptor protein that does not act directly in DNA repair. Instead, it recruits other proteins to the sites of DNA breaks to facilitate NHEJ repair, which then compete with BRCA1-dependent HR-mediated DNA repair. In support of this hypothesis, several groups demonstrated that RIF1 and PTIP are key factors that act downstream of 53BP1 and counteract BRCA1's functions in DNA repair (10–15). However, RIF1 and PTIP have no known enzymatic activity in DNA repair and rather, may serve as a scaffold for the recruitment of other DSB-processing enzymes in this pathway. Recently, we and others reported that downstream of 53BP1, Artemis and MDA2L2 are crucial in coordinating pathologic DSB repair pathway choices in BRCA1-deficient cells. Loss of Artemis or MAD2L2 restores PARPi resistance in BRCA1-deficient cells (16–18). More recently, the Shieldin complex was found to act as the downstream effector of 53BP1/RIF1/MAD2L2 to restrict DSB resection and counteract HR (19–24). Thus, 53BP1 controls two downstream pathways, one mediated by PTIP and Artemis and the other by RIF1 and MAD2L2/Shieldin, to promote NHEJ and suppress HR repair.

Although 53BP1 has been extensively investigated for its downstream pathways and DNA repair pathway choice, little is known about upstream regulation of 53BP1 function in DNA repair. In particular, it remains unclear how post-translational modification of 53BP1 affects DSB repair. We and others recently showed that TIRR (Tudor interacting repair regulator) directly binds to the 53BP1 Tudor domain, masks its binding surface for H4K20me2, and regulates 53BP1 functions *in vivo* (25–29). Given that the TIRR homolog, Nudix enzyme NUDT16, has been shown to have *in vitro* hydrolase activities that remove protein ADP-ribosylation (30), we investigated whether NUDT16 regulates 53BP1 stability and we are now reporting that by hydrolyzing PAR chains on 53BP1, NUDT16 indeed regulates 53BP1 stability.

MATERIALS AND METHODS

Cell culture and plasmids

HEK293T, MCF10A, and MDA-MB-231 cells were purchased from the ATCC and cultured under conditions specified by the ATCC. All cell lines were cultured within 20 passages prior to use. They were authenticated by short tandem repeat profiling and were tested to ensure absence of *Mycoplasma* by PCR analysis. NUDT16 cDNA was subcloned into plasmid pDONR201 as the entry vector and subsequently transferred to gateway-compatible destination vectors for the expression of SFB, Myc, HA, GST, or MBP epitope-tagged fusion proteins.

Antibodies

Anti-TIRR antibody development has been described previously (25). Monoclonal anti-FLAG M2 (#F3165), anti-MBP (#AB3596), and anti-β-actin (#A5441) antibodies were purchased from Sigma. Anti-Myc (#sc-40), anti-GAPDH (#sc-47724), and anti-GST (#sc-138) antibodies were obtained from Santa Cruz. Anti-PAR (#4335-MC-50) and anti-PARP1 (#4338-MC-50) antibodies were purchased from Trevigen. Anti-HA (#PI26183) was obtained from Fisher Scientific, and anti-NUDT16 (#12889–1-AP) was purchased from Proteintech Group. Anti-53BP1 (#4937S), anti-phospho-Chk2 (T68) (#2661S) were obtained from Cell Signaling Technology. Anti-phospho-RPA2 (S4/S8) (#A300–245A) was purchased from Bethyl Laboratories.

Immunofluorescence staining

Cells grown on coverslips were mock-treated or irradiated using a JL Shepherd Cs137 source (20 Gy) and allowed to recover for 4 hours. Cells were fixed in 3% paraformaldehyde solution for 10 minutes and then permeabilized in 0.5% Triton X-100-PBS for 5 minutes at room temperature. Cells were then incubated with primary antibodies (anti-FLAG, and anti-53BP1) diluted in 5% goat serum for 1 hour at room temperature. Coverslips were washed and incubated either with rhodamine or FITC conjugated secondary antibodies for 1 hour at room temperature. Cells were then stained with DAPI to visualize nuclear DNA. The coverslips were mounted on glass slides with an anti-fade agent and evaluated using a Nikon Eclipse E800 fluorescence microscope.

Co-immunoprecipitation and Western blotting

Cells were lysed with NTEN buffer (20mM Tris-HCl, pH 8.0, 100mM NaCl, 1 mM EDTA, 0.5% Nonidet P-40) containing pepstatin A and aprotinin on ice for 30 minutes. Clear cell lysates were incubated with either protein A/G-agarose beads coupled with anti-53BP1 antibody (#A700–011, Bethyl) or streptavidin beads (#17511301, Fisher Scientific) for 3 hours at 4°C. Beads were then washed 4 times with NTEN buffer and boiled in 2xLaemmli buffer, and proteins were separated by SDS-PAGE. PVDF membranes were blocked in 5% milk in TBST buffer and then probed with antibodies as indicated.

Clonogenic survival assays

An ionizing radiation (IR) sensitivity assay was carried out as described previously (25). Briefly, a total of 1×10^3 cells was seeded onto 60-mm dishes in triplicate and treated with IR at the indicated doses the next day. Cells were then incubated for 14 days. Resulting colonies were fixed and stained with Coomassie Blue. Colony numbers were counted using a GelDoc system with Quantity One software (version 2.0, Bio-Rad). Results were summarized as the mean of data obtained from three independent experiments.

In vitro PARylation assays

HEK293T cells were transfected with plasmids encoding SFB-tagged proteins. Cells were lysed with NTEN buffer containing pepstatin A and aprotinin on ice for 30 minutes. Clear cell lysates were incubated with streptavidin beads at 4°C for 3 hours. Then the beads were eluted with 2 mg/ml biotin in NTEN buffer at 4°C for 2 hours. *In vitro* PARylation assays were performed in a reaction mix consisting of the eluates, 1x reaction buffer (0.5M Tris/HCl pH 8.0, 0.04M MgCl2, 0.5M NaCl, 2 mM DTT), 20μM NAD+, 1xactive DNA for 30 minutes at room temperature. The reaction mixture was terminated with 2xLaemmli buffer and subjected to SDS–PAGE. PARP1 enzyme served as a positive control in a reaction mix without eluates or streptavidin beads coated with SFB-tagged proteins.

Comet assay

A comet assay was performed for the indicated cells treated with IR (2Gy). Cells were mixed with 250μl low-melting agarose and were placed on microscope slides with frosted ends. The slides were immersed in a cooled lysing solution (10% DMSO, 1% Triton X-100, 2.5M NaCl, 100mM EDTA and 10mM Tris, pH10) for 24 hours at 4°C. All steps after lysis were performed under dim light to prevent additional DNA damage. The DNA was allowed to unwind for 1 hour in alkaline unwinding buffer (300mM NaOH and 1mM EDTA, pH13). Electrophoresis was performed at 25 V and 300 mA for 20 minutes. Slides were then sprayed with neutralization buffer, pH7.5. Ethidium bromide (60μl, 1.5 μg/ml) was added to each slide, and a cover glass was placed on the gel. The DNA migration was analyzed using a Leica plus 60 microscopy with fluorescence (filter 12) and measured with a scaled ocular. To evaluate DNA migration (tail length), 50 cells were scored on each slide and triplicated for each dose. Three independent experiments were performed.

RESULTS

NUDT16 regulates 53BP1 stability

TIRR and NUDT16 belong to the family of nucleoside diphosphate-linked moiety X (Nudix) hydrolases. Nudix proteins are characterized by a highly conserved 23-amino acid Nudix motif (Nudix box), GX5EX7REUXEEXGU (Figure 1A), where U is an aliphatic or hydrophobic residue(31). TIRR is required for 53BP1 stability (25,26). Given that NUDT16 is structurally similar to TIRR, we speculate that NUDT16 may have functions similar to TIRR. We generated NUDT16 knockout (KO) cells by CRISPR/Cas9 editing. Similar to TIRR KO, loss of NUDT16 decreased 53BP1 protein levels (Figure 1B), suggesting that NUDT16 is required for 53BP1 stability. The 53BP1 protein level was further decreased in

TIRR/NUDT16 double KO cells compared with NUDT16 KO or TIRR KO cells (Figure 1B), indicating that TIRR and NUDT16 might have synergistic effect on 53BP1 protein stability. Moreover, the 53BP1 protein decrease was indeed due to loss of NUDT16 because the expression of sgRNA-resistant wild-type NUDT16 restored the 53BP1 protein level in NUDT16-depleted MDA-MB-231 cells (Figure 1C).

NUDT16 removes 53BP1 ADP-ribosylation

NUDT16 has been shown recently to have *in vitro* activities that remove protein ADP-ribosylation (30). Because TIRR and NUDT16 share the highly conserved Nudix motif (Figure 1A), we performed an *in vitro* ADP-ribosylation assay to determine whether both TIRR and NUDT16 have hydrolyzing activity that cleaves protein ADP-ribosylation. Surprisingly, NUDT16, but not TIRR, could remove the ADP-ribosylation of PARP1 (Figure 2A). Next, we attempted to identify the conserved key residues in the Nudix motif of NUDT16 that are responsible for the hydrolase activity that removes PAR chains. We generated a NUDT16 E>Q mutant (E76QE79QE80Q) (32) and performed an *in vitro* PARylation assay. As shown in Figure 2B, the E>Q mutant of NUDT16 failed to remove the PAR chain from PARP1, indicating that the E76E79E80 residues within the Nudix motif are catalytically active residues required for NUDT16 hydrolase activity.

Given that PARP1 is activated at sites of DNA breaks and promotes ADP-ribosylation of itself and other DNA repair proteins (33), it is reasonable to speculate that NUDT16 hydrolase activity may be important for its function in 53BP1 regulation and specifically in regulating ADP-ribosylation of 53BP1. We first determined whether 53BP1 is ADP-ribosylated and whether NUDT16 would affect 53BP1 ADP-ribosylation *in vitro*. As shown in Figure 2C, only 53BP1 C terminus (CT, 1043–1972aa) is ADP-ribosylated, although the same condition also applied to 53BP1 N terminus (NT, 1–1042aa). Furthermore, PARP1 protein was not detected in eluates before or after *in vitro* PARylation assay (Figure 2C; Supplemental Figure S1A and S1B), suggesting that the PAR signals are linked to 53BP1 CT. Importantly, NUDT16 removed the PAR chain from 53BP1 CT (Figure 2D), suggesting that NUDT16 has hydrolyzing activity that cleaves ADP-ribosylation of 53BP1 CT. It is difficult to predict and identify the poly-ribosylation sites because protein ADP-ribosylation is a heterogeneous, highly charged, and rapidly degrading post-translational modification. We performed an *in vitro* PARylation assay using a series of truncation mutants and internal deletion mutants of 53BP1 and found that fragment F2 (1455–1557aa) was ADP-ribosylated (Figure 2E). Fragment F2 was aligned among species, and multiple conserved Glu (E) and Asp (D) residues were identified. We generated a series of multi-point mutants for these conserved Glu (E) and Asp (D) residues and performed an *in vitro* PARylation assay. We found that the 53BP1 M2 mutant, but not other mutants, greatly diminished PAR chain proteins (Figure 2F–2H), suggesting that the D1520D1521E1524D1526 residues are ribosylation sites involved in the ADP-ribosylation of 53BP1.

DNA damage-induced 53BP1 ADP-ribosylation leads to ubiquitination and degradation

Recent studies demonstrate that ADP-ribosylation can signal for ubiquitination and promote the degradation of ADP-ribosylated proteins (34–37). Given that ADP-ribosylation can prime ubiquitination at DNA lesions, we investigated the regulation of 53BP1 protein levels

during DNA damage. We found that after IR, 53BP1 protein levels decreased in the cytoplasmic fraction in MCF10A cells, and further decreased in NUDT16 KO cells (Figure 3A). Similar results were obtained in MDA-MB-231 breast cancer cells NUDT16 KO and in HeLa cells with NUDT16 knockdown (KD) (Supplemental Figure S2). Furthermore, we observed that after IR, 53BP1 level decreased in the cytoplasmic fraction in a time-dependent manner (Figure 3B), suggesting that 53BP1 is unstable in the cytoplasmic fraction after DNA damage, possibly due to 53BP1 ADP-ribosylation-dependent ubiquitination and degradation. To further determine whether 53BP1 is ADP-ribosylated *in vivo*, 53BP1 was immunoprecipitated with anti-53BP1 antibody, followed by immunoblotting with an antibody to PAR. We observed that 53BP1 is indeed ADP-ribosylated *in vivo*, and ADP-ribosylated 53BP1 is markedly increased after IR. As a control, we treated cells with a PARPi (olaparib) to prevent ADP-ribosylation of 53BP1 (Figure 3C). Because NUDT16 has hydrolyzing activity that allows it to remove protein ADP-ribosylation, we determined whether 53BP1 ADP-ribosylation is increased in NUDT16 KO cells. We immunoprecipitated PARylated proteins with anti-PAR antibody, followed by immunoblotting with 53BP1 antibody in MCF10A cells and its derivative NUDT16 KO cells. We found that ADP-ribosylated 53BP1 is markedly increased in NUDT16 KO cells and decreased after IR (Figure 3D), suggesting that NUDT16 has hydrolyzing activity that removes ADP-ribosylation of 53BP1 *in vivo*. PARPi are used to inhibit PARP enzymatic activity to serve as the major barrier to ADP-ribosylation. As shown in Figure 3E, cells were treated with PARPi in the absence or presence of IR. 53BP1 protein slightly increased after PARPi treatment. Moreover, after treatment with PARPi, 53BP1 protein was partially rescued following IR, indicating that PARPi blocked the IR-induced decrease in 53BP1. In addition, because the basal level of 53BP1 ubiquitination is low, a mild decrease in 53BP1 ubiquitination was detected after PARPi treatment alone. Although 53BP1 ubiquitination was increased in response to IR, PARPi treatment led to decreased 53BP1 ubiquitination after IR (Figure 3E), suggesting that ADP-ribosylated 53BP1 mediates its own ubiquitination and degradation.

The E3 ligase RNF146 is required for ADP-ribosylation-dependent ubiquitination and degradation of 53BP1

The relationship between ADP-ribosylation and ubiquitination has been well described for the RING-type E3 ubiquitin ligase, RNF146, which is responsible for ADP-ribosylation-dependent ubiquitination. RNF146 contains two conserved domains, a RING domain that is likely an E3 ubiquitin ligase, and a WWE domain that is a PAR-binding domain (38–41). We tested whether RNF146 also acts as an E3 ubiquitin ligase for ADP-ribosylated 53BP1. Expression of wild-type RNF146 led to reduced 53BP1 protein (full length and CT), which was completely reversed by the proteasome inhibitor MG132; in contrast, RNF146ΔWWE or RNF146ΔRING deletion mutants had no effect on 53BP1 protein level (Figure 4A and 4B), suggesting that 53BP1 needs to be ADP-ribosylated before RNF146 can recognize it for ubiquitination and degradation. Indeed, only wild-type RNF146 promoted the ubiquitination of 53BP1 (Figure 4C), indicating that both the PAR recognition domain (WWE) and the E3 ligase activity domain (RING) of RNF146 are required for RNF146-mediated 53BP1 ubiquitination and degradation. To determine the effect of the ADP-ribosylated residues of 53BP1 on RNF146 mediated 53BP1 ubiquitination and degradation,

we co-transfected the M2 mutant of 53BP1 (full length and CT) with RNF146 wild-type, RNF146ΔWWE, or RNF146ΔRING deletion mutants. RNF146 failed to facilitate the degradation of the M2 mutant of 53BP1 (full length and CT) (Figure 4D; Supplemental Figure S3A), again supporting the idea that RNF146-mediated 53BP1 ubiquitination and degradation depend on the ADP-ribosylation of 53BP1. We also performed cycloheximide treatment experiments and showed that the half-life of wild-type 53BP1 CT was significantly shorter than that of the M2 mutant of 53BP1 CT in MCF10A cells regardless of whether NUDT16 was intact, indicating that loss of ADP-ribosylation of 53BP1 enhances 53BP1 protein stability (Figure 4E; Supplemental Figure S3B). In addition, as shown in Supplemental Figure 3C, the protein level for wild-type of 53BP1 CT increased after PARPi treatment, but dramatically decreased after IR treatment in both MCF10A and NUDT16 KO cells with reconstitution of wild-type of 53BP1 CT. However, the protein level for the M2 mutant of 53BP1 CT was stable in both MCF10A and NUDT16 KO cells reconstituted with the M2 mutant of 53BP1 CT, suggesting that 53BP1 stability depends on the 53BP1 ADP-ribosylation-dependent ubiquitination and degradation. To address whether RNF146 regulates degradation of 53BP1 and whether NUDT16 is involved in this process, we depleted endogenous RNF146 in both MCF10A and NUDT16 KO cells. We observed that depletion of endogenous RNF146 led to 53BP1 stabilization (Figure 4F), suggesting that NUDT16 loss promotes ADP-ribosylation of 53BP1, which in turn leads to its ubiquitination and degradation by the E3 ligase RNF146.

NUDT16 hydrolase activity is required for 53BP1 protein stability

Given that the E76E79E80 residues within the Nudix motif are catalytically active residues required for NUDT16 hydrolase activity, we wanted to know whether a catalytically inactive mutant affects 53BP1 protein levels. The expression of sgRNA-resistant wild-type NUDT16 restored 53BP1 protein levels in MCF10A-derived NUDT16 KO cells, whereas expression of the E>Q mutant of NUDT16 failed to do so, indicating that the hydrolase activity of NUDT16 is critical to stabilizing 53BP1 protein (Figure 5A). Similar results were observed in NUDT16 KO of MDA-MB-231 breast cancer cells with reconstitution of wild-type NUDT16 and E>Q mutant of NUDT16 (Figure 5B). In agreement with the results from Figure 3A, the restored 53BP1 protein levels decreased after IR in NUDT16 KO cells that have reconstitution of wild-type NUDT16 after IR (Figure 5C). Because NUDT16 depletion reduced 53BP1 expression, we anticipate that NUDT16 loss should also lead to PARPi resistance in BRCA1 deficient cells, which is supported by our experimental data shown in Figure 5D. Furthermore, reconstitution of wild-type NUDT16 re-sensitized cells to PARPi, whereas reconstitution with the hydrolase-inactive mutant (E>Q) of NUDT16 failed to do so (Figure 5D), suggesting that NUDT16 and its hydrolase activity are critical not only for 53BP1 expression but also for antagonizing BRCA1-mediated DNA repair.

NUDT16 hydrolase activity alters 53BP1 localization at DNA damage sites

Although 53BP1 foci formation is not affected by overexpression of wild-type NUDT16, the E>Q mutant of NUDT16 partially prevents the localization of 53BP1 to sites of DNA damage in NUDT16 KO of MCF10A cells (Figure 6A), indicating that the catalytic activity of NUDT16 affects the recruitment of 53BP1 to DSBs. Similar results were obtained in NUDT16 KO of MDA-MB-231 breast cancer cells (Figure 6B). Because we and others

previously reported that TIRR overexpression inhibits 53BP1 foci at DSBs in cells (25–29), we examined whether the E>Q mutant of NUDT16 is associated with TIRR. Interestingly, we observed that, unlike wild-type NUDT16, the NUDT16 E>Q mutant strongly binds to TIRR (Figure 6C and 6D). Furthermore, the amount of NUDT16 E>Q mutant bound with TIRR increases after IR (Figure 6E). Moreover, in the presence of NUDT16 E>Q mutant, the binding of TIRR and 53BP1 Tudor-UDR increased by ~ two-fold (Figure 6F), suggesting that NUDT16 E>Q mutant could enhance binding of 53BP1 Tudor-UDR to TIRR. Next, to determine whether NUDT16 E>Q directly affects binding of the 53BP1 Tudor-UDR to H4K20me2, we performed a biotin-H4K20me2 peptide pulldown assay and showed that the NUDT16 E>Q mutant impaired the binding of the 53BP1 Tudor-UDR domain to an H4K20me2 peptide (Figure 6G). Taken together, our results provide evidence that the NUDT16 E>Q mutant is involved in recruiting 53BP1 to DNA damage sites.

NUDT16 regulates 53BP1 ADP-ribosylation in the DNA damage response.

It is established that 53BP1 is involved in the DNA damage response (42). NUDT16 also likely participates in the DNA damage response because NUDT16 regulates 53BP1 stability. A comet assay revealed that MCF10A-derived NUDT16 KO cells had a significantly increased tail in three independent experiments (Figure 7A), suggesting that loss of NUDT16 caused an accumulation of DNA strand breaks that could not be repaired. In response to DNA damage, multiple target proteins are phosphorylated, including RPA2 and Chk2. As shown in Figure 7B, NUDT16 KO cells had a clearly reduced capacity to phosphorylate RPA2 (S4/S8) and Chk2 (T68) following IR. After treatment with PARPi, phosphorylation of RPA2 (S4/S8) and Chk2 (T68) was partially rescued in response to IR, indicating that PARPi could rescue the DNA repair defects induced by loss of NUDT16. 53BP1 is required for cell survival after IR (42). Because NUDT16 regulates 53BP1 stability, we anticipated that NUDT16 loss should also lead to IR sensitivity, which was the case as shown by cell survival data in Figure 7C. Similar data were also obtained in NUDT16 KO in MDA-MB-231 cells (Supplemental Figure S4A). Furthermore, expression of gRNA-resistant wild-type NUDT16 decreased IR sensitivity in MCF10A or MDA-MB-231 cells with NUDT16 knockout, but reconstitution with the E>Q mutant of NUDT16 failed to do so (Figure 7D; Supplemental Figure S4B). These data suggest that the NUDT16 hydrolase activity is required for cell survival in response to DNA damage. Together, these data indicate that NUDT16 plays an important role in the DNA damage response.

To demonstrate the role of ADP-ribosylation of 53BP1 in DNA damage response, we first detected the γH2AX signal in MCF10A and NUDT16 KO cells after IR. In response to DNA damage, the γH2AX signal increased and then diminished along with the DNA repair process. However, loss of NUDT16 impaired the capacity to diminish γH2AX signal following IR, indicating that NUDT16 participates in the DNA damage response (Supplemental Figure S5A). To further understand the role of the M2 mutant (de-ADP-ribosylation) of 53BP1 CT in DNA repair, we generated NUDT16 KO cells that were reconstituted with wild-type or M2 mutant of 53BP1 CT. As shown in Supplemental Figure S5A, the induced γH2AX signal was decreased in NUDT16 KO cells reconstituted with wild-type of 53BP1 CT after 8 hours of IR, whereas the γH2AX signal was much more stable in NUDT16 KO cells reconstituted with the M2 mutant of 53BP1 CT, suggesting that

M2 mutant is not able to rescue the repair defects of NUDT16 KO cells present after DNA damage.

DISCUSSION

Various lines of evidence show that BRCA1 or BRCA2 dysfunction profoundly sensitizes cells to PARP inhibitors due to HR repair defects in BRCA1- or BRCA2-deficient cancer cells (43–46). However, PARPi resistance is a major clinical problem in BRCA1/2-mutated cancers. Unexpectedly, loss of the DNA repair protein 53BP1 renders BRCA1-deficient cancer cells resistant to PARPi treatment (47,48), indicating that loss of 53BP1 expression is at least one scenario by which therapeutic resistance may arise in BRCA-mutated cancers. 53BP1 is a DNA damage response protein that participates in DNA damage checkpoint control as well as in DNA repair. We and others reported recently that mechanistically, 53BP1 acts as an adaptor protein and controls two downstream sub-pathways, one mediated by PTIP and Artemis and the other mediated by RIF1 and MAD2L2/Shieldin, to coordinate pathologic DSB repair pathway choices (10–24). These studies uncovered events downstream of 53BP1 that are important for DNA repair. However, the upstream regulator(s) of 53BP1 function in DNA repair and cellular response to PARPi in BRCA-mutated cancers remain unknown.

Recent work reported by us and others revealed that TIRR (also called NUDT16L1) stabilizes 53BP1 and prevents 53BP1 localization to sites of DNA breaks by masking its H4K20me2-binding surface (25–29). The work we report here has revealed that the TIRR homolog, Nudix hydrolase NUDT16 can remove ADP-ribosylated 53BP1 *in vivo* and *in vitro*. In addition, similar to TIRR, NUDT16 loss destabilizes and thus decreases the 53BP1 protein level, which may be due to 53BP1 degradation mediated by ubiquitination. Recent studies demonstrate that ADP-ribosylation can signal for ubiquitination and promote the degradation of ADP-ribosylated proteins (34–37). Our current working model is that ADP-ribosylation is a previously unknown post-translational modification of 53BP1 that is increased in response to DNA damage. The ADP-ribosylated 53BP1 is targeted by a PAR-binding E3 ubiquitin ligase, RNF146, leading to 53BP1 ubiquitination and degradation (Figure 7E). Under normal conditions, NUDT16 has hydrolyzing activity that cleaves ADP-ribosylation of 53BP1 and inhibits 53BP1 ubiquitination and degradation, stabilizing 53BP1 protein and allowing its recruitment to methylated histones. In the presence of DNA damage, NUDT16 does not affect 53BP1 recruitment to DSBs.

Our data also revealed intriguing results under potential pathological conditions (*e.g.*, NUDT16 mutations) by engineering two types of cell lines across a wide range of origins, which are either NUDT16 knockout or overexpress a NUDT16 catalytic inactive mutant (E>Q). We showed that the level of 53BP1 protein was dramatically decreased when loss of NUDT16 or overexpression of a NUDT16 catalytic inactive mutant. We further observed that NUDT16 loss or NUDT16 catalytic inactive mutant promotes ADP-ribosylation of 53BP1, which in turn leads to its ubiquitination and degradation. We and others have reported that TIRR binds to the 53BP1 Tudor domain and masks 53BP1 Tudor binding site for H4K20me2, thereby inhibiting 53BP1 accumulation at DNA damage sites and preventing formation of nuclear foci (25–29). Surprisingly, NUDT16 catalytic inactive

mutant partially prevents the localization of 53BP1 to sites of DNA damage, suggesting that the catalytic activity of NUDT16 affects the recruitment of 53BP1 to DSBs. To elucidate the mechanism underlying the loss of catalytic activity of NUDT16 on 53BP1 recruitment at DSBs, we showed that the catalytic inactive mutant of NUDT16 impaired binding between the 53BP1 Tudor domain and H4K20me2. Our data provide evidence that the catalytic inactive mutant of NUDT16 inhibits 53BP1 recruitment to DNA damage sites (Figure 7E).

NUDT16 shares a high sequence homology and overall structural similarity with TIRR. Both NUDT16 and TIRR regulate 53BP1 stability in the nucleosome fraction. However, in contrast to TIRR, NUDT16 has at least two different, unique functions. First, NUDT16, but not TIRR, has hydrolase activities that remove ADP-ribosylation from 53BP1. Second, overexpression of NUDT16 does not affect 53BP1 foci formation after irradiation, whereas TIRR overexpression inhibits 53BP1 localization to DSBs by blocking its H4K20me2-binding sites. Although structure-based sequence alignments showed that NUDT16 has high sequence similarity with TIRR, a number of residues in NUDT16 are crucial and specific for NUDT16 function. Recently, we and others revealed that a TIRR histidine residue is responsible for 53BP1 Tudor domain binding, and this residue is not present in NUDT16 (27–29). *Vice versa*, we speculate that one or several residues in NUDT16 that are not present in TIRR will be largely responsible for its diverse functions.

The Nudix hydrolase activity of NUDT16 has been implicated in ADP-ribose metabolism. Data extracted from cBioportal (http://www.cBioportal.org) shows that 32 of 35 cancer types exhibit NUDT16 gene amplification (Supplemental Figure S6). Therefore, NUDT16 hydrolase inhibitors are expected to possess anti-cancer therapeutic potential. If we understand both up- and downstream regulation of 53BP1, then we will know mechanistically how the 53BP1 repair pathway operates in the cell to facilitate DNA repair, opening new targets for improving cancer therapy and overcoming therapeutic resistance.

Supplementary Material

Refer to Web version on PubMed Central for supplementary material.

Acknowledgments

We would like to thank all our colleagues in the Gong laboratory for insightful discussion and technical assistance. Myc-RNF146 WT and mutants were kindly provided by Drs. Junjie Chen and Nan Li (University of Texas MD Anderson Cancer Center). We also want to thank Dr. Youwei Zhang and Dr. George Stark for valuable comments and suggestions. We thank Dr. Cassandra Talerico for critical reading of the manuscript. This work was supported by National Institutes of Health Grant (R01CA222195 to Z.Gong. and RO1CA184137 to A.Almasan), Ovarian Cancer Research Fund Alliance Grant 373376 and 605161 (Z.Gong). This work was also in part supported by Center of Research Excellence in Gynecologic Cancer and VeloSano Pilot Award.

REFERENCES

1. Botuyan MV, Lee J, Ward IM, Kim JE, Thompson JR, Chen J, et al. Structural basis for the methylation state-specific recognition of histone H4–K20 by 53BP1 and Crb2 in DNA repair. Cell 2006;127:1361–73 [PubMed: 17190600]
2. Pei H, Zhang L, Luo K, Qin Y, Chesi M, Fei F, et al. MMSET regulates histone H4K20 methylation and 53BP1 accumulation at DNA damage sites. Nature 2011;470:124–8 [PubMed: 21293379]

3. Fradet-Turcotte A, Canny MD, Escribano-Diaz C, Orthwein A, Leung CC, Huang H, et al. 53BP1 is a reader of the DNA-damage-induced H2A Lys 15 ubiquitin mark. Nature 2013;499:50–4 [PubMed: 23760478]
4. Celeste A, Fernandez-Capetillo O, Kruhlak MJ, Pilch DR, Staudt DW, Lee A, et al. Histone H2AX phosphorylation is dispensable for the initial recognition of DNA breaks. Nat Cell Biol 2003;5:675–9 [PubMed: 12792649]
5. Doil C, Mailand N, Bekker-Jensen S, Menard P, Larsen DH, Pepperkok R, et al. RNF168 binds and amplifies ubiquitin conjugates on damaged chromosomes to allow accumulation of repair proteins. Cell 2009;136:435–46 [PubMed: 19203579]
6. Huen MS, Grant R, Manke I, Minn K, Yu X, Yaffe MB, et al. RNF8 transduces the DNA-damage signal via histone ubiquitylation and checkpoint protein assembly. Cell 2007;131:901–14 [PubMed: 18001825]
7. Kolas NK, Chapman JR, Nakada S, Ylanko J, Chahwan R, Sweeney FD, et al. Orchestration of the DNA-damage response by the RNF8 ubiquitin ligase. Science 2007;318:1637–40 [PubMed: 18006705]
8. Mailand N, Bekker-Jensen S, Faustrup H, Melander F, Bartek J, Lukas C, et al. RNF8 ubiquitylates histones at DNA double-strand breaks and promotes assembly of repair proteins. Cell 2007;131:887–900 [PubMed: 18001824]
9. Stewart GS, Panier S, Townsend K, Al-Hakim AK, Kolas NK, Miller ES, et al. The RIDDLE syndrome protein mediates a ubiquitin-dependent signaling cascade at sites of DNA damage. Cell 2009;136:420–34 [PubMed: 19203578]
10. Callen E, Di Virgilio M, Kruhlak MJ, Nieto-Soler M, Wong N, Chen HT, et al. 53BP1 mediates productive and mutagenic DNA repair through distinct phosphoprotein interactions. Cell 2013;153:1266–80 [PubMed: 23727112]
11. Chapman JR, Barral P, Vannier JB, Borel V, Steger M, Tomas-Loba A, et al. RIF1 is essential for 53BP1-dependent nonhomologous end joining and suppression of DNA double-strand break resection. Mol Cell 2013;49:858–71 [PubMed: 23333305]
12. Di Virgilio M, Callen E, Yamane A, Zhang W, Jankovic M, Gitlin AD, et al. Rif1 prevents resection of DNA breaks and promotes immunoglobulin class switching. Science 2013;339:711–5 [PubMed: 23306439]
13. Escribano-Diaz C, Orthwein A, Fradet-Turcotte A, Xing M, Young JT, Tkac J, et al. A cell cycle-dependent regulatory circuit composed of 53BP1-RIF1 and BRCA1-CtIP controls DNA repair pathway choice. Mol Cell 2013;49:872–83 [PubMed: 23333306]
14. Feng L, Fong KW, Wang J, Wang W, Chen J. RIF1 counteracts BRCA1-mediated end resection during DNA repair. J Biol Chem 2013;288:11135–43 [PubMed: 23486525]
15. Zimmermann M, Lottersberger F, Buonomo SB, Sfeir A, de Lange T. 53BP1 regulates DSB repair using Rif1 to control 5' end resection. Science 2013;339:700–4 [PubMed: 23306437]
16. Boersma V, Moatti N, Segura-Bayona S, Peuscher MH, van der Torre J, Wevers BA, et al. MAD2L2 controls DNA repair at telomeres and DNA breaks by inhibiting 5' end resection. Nature 2015;521:537–40 [PubMed: 25799990]
17. Wang J, Aroumougame A, Lobrich M, Li Y, Chen D, Chen J, et al. PTIP associates with Artemis to dictate DNA repair pathway choice. Genes Dev 2014;28:2693–8 [PubMed: 25512557]
18. Xu G, Chapman JR, Brandsma I, Yuan J, Mistrik M, Bouwman P, et al. REV7 counteracts DNA double-strand break resection and affects PARP inhibition. Nature 2015;521:541–4 [PubMed: 25799992]
19. Dev H, Chiang TW, Lescale C, de Krijger I, Martin AG, Pilger D, et al. Shieldin complex promotes DNA end-joining and counters homologous recombination in BRCA1-null cells. Nat Cell Biol 2018;20:954–65 [PubMed: 30022119]
20. Ghezraoui H, Oliveira C, Becker JR, Bilham K, Moralli D, Anzilotti C, et al. 53BP1 cooperation with the REV7-shieldin complex underpins DNA structure-specific NHEJ. Nature 2018
21. Gupta R, Somyajit K, Narita T, Maskey E, Stanlie A, Kremer M, et al. DNA Repair Network Analysis Reveals Shieldin as a Key Regulator of NHEJ and PARP Inhibitor Sensitivity. Cell 2018;173:972–88 e23 [PubMed: 29656893]

22. Mirman Z, Lottersberger F, Takai H, Kibe T, Gong Y, Takai K, et al. 53BP1-RIF1-shieldin counteracts DSB resection through CST- and Polalpha-dependent fill-in. Nature 2018
23. Noordermeer SM, Adam S, Setiaputra D, Barazas M, Pettitt SJ, Ling AK, et al. The shieldin complex mediates 53BP1-dependent DNA repair. Nature 2018
24. Tomida J, Takata KI, Bhetawal S, Person MD, Chao HP, Tang DG, et al. FAM35A associates with REV7 and modulates DNA damage responses of normal and BRCA1-defective cells. The EMBO journal 2018;37
25. Zhang A, Peng B, Huang P, Chen J, Gong Z. The p53-binding protein 1-Tudor-interacting repair regulator complex participates in the DNA damage response. J Biol Chem 2017;292:6461–7 [PubMed: 28213517]
26. Drane P, Brault ME, Cui G, Meghani K, Chaubey S, Detappe A, et al. TIRR regulates 53BP1 by masking its histone methyl-lysine binding function. Nature 2017;543:211–6 [PubMed: 28241136]
27. Dai Y, Zhang A, Shan S, Gong Z, Zhou Z. Structural basis for recognition of 53BP1 tandem Tudor domain by TIRR. Nat Commun 2018;9:2123 [PubMed: 29844495]
28. Botuyan MV, Cui G, Drane P, Oliveira C, Detappe A, Brault ME, et al. Mechanism of 53BP1 activity regulation by RNA-binding TIRR and a designer protein. Nat Struct Mol Biol 2018;25:591–600 [PubMed: 29967538]
29. Wang J, Yuan Z, Cui Y, Xie R, Yang G, Kassab MA, et al. Molecular basis for the inhibition of the methyl-lysine binding function of 53BP1 by TIRR. Nat Commun 2018;9:2689 [PubMed: 30002377]
30. Palazzo L, Thomas B, Jemth AS, Colby T, Leidecker O, Feijs KL, et al. Processing of protein ADP-ribosylation by Nudix hydrolases. Biochem J 2015;468:293–301 [PubMed: 25789582]
31. McLennan AG. The Nudix hydrolase superfamily. Cell Mol Life Sci 2006;63:123–43 [PubMed: 16378245]
32. Taylor MJ, Peculis BA. Evolutionary conservation supports ancient origin for Nudt16, a nuclear-localized, RNA-binding, RNA-decapping enzyme. Nucleic Acids Res 2008;36:6021–34 [PubMed: 18820299]
33. Gibson BA, Kraus WL. New insights into the molecular and cellular functions of poly(ADP-ribose) and PARPs. Nat Rev Mol Cell Biol 2012;13:411–24 [PubMed: 22713970]
34. Guettler S, LaRose J, Petsalaki E, Gish G, Scotter A, Pawson T, et al. Structural basis and sequence rules for substrate recognition by Tankyrase explain the basis for cherubism disease. Cell 2011;147:1340–54 [PubMed: 22153077]
35. Huang SM, Mishina YM, Liu S, Cheung A, Stegmeier F, Michaud GA, et al. Tankyrase inhibition stabilizes axin and antagonizes Wnt signalling. Nature 2009;461:614–20 [PubMed: 19759537]
36. Levaot N, Voytyuk O, Dimitriou I, Sircoulomb F, Chandrakumar A, Deckert M, et al. Loss of Tankyrase-mediated destruction of 3BP2 is the underlying pathogenic mechanism of cherubism. Cell 2011;147:1324–39 [PubMed: 22153076]
37. Li N, Zhang Y, Han X, Liang K, Wang J, Feng L, et al. Poly-ADP ribosylation of PTEN by tankyrases promotes PTEN degradation and tumor growth. Genes Dev 2015;29:157–70 [PubMed: 25547115]
38. DaRosa PA, Wang Z, Jiang X, Pruneda JN, Cong F, Klevit RE, et al. Allosteric activation of the RNF146 ubiquitin ligase by a poly(ADP-ribosyl)ation signal. Nature 2015;517:223–6 [PubMed: 25327252]
39. Kang HC, Lee YI, Shin JH, Andrabi SA, Chi Z, Gagne JP, et al. Iduna is a poly(ADP-ribose) (PAR)-dependent E3 ubiquitin ligase that regulates DNA damage. Proc Natl Acad Sci U S A 2011;108:14103–8 [PubMed: 21825151]
40. Wang Z, Michaud GA, Cheng Z, Zhang Y, Hinds TR, Fan E, et al. Recognition of the iso-ADP-ribose moiety in poly(ADP-ribose) by WWE domains suggests a general mechanism for poly(ADP-ribosyl)ation-dependent ubiquitination. Genes Dev 2012;26:235–40 [PubMed: 22267412]
41. Zhang Y, Liu S, Mickanin C, Feng Y, Charlat O, Michaud GA, et al. RNF146 is a poly(ADP-ribose)-directed E3 ligase that regulates axin degradation and Wnt signalling. Nat Cell Biol 2011;13:623–9 [PubMed: 21478859]

42. Ward IM, Minn K, van Deursen J, Chen J. p53 Binding protein 53BP1 is required for DNA damage responses and tumor suppression in mice. Mol Cell Biol 2003;23:2556–63 [PubMed: 12640136]
43. Audeh MW, Carmichael J, Penson RT, Friedlander M, Powell B, Bell-McGuinn KM, et al. Oral poly(ADP-ribose) polymerase inhibitor olaparib in patients with BRCA1 or BRCA2 mutations and recurrent ovarian cancer: a proof-of-concept trial. Lancet 2010;376:245–51 [PubMed: 20609468]
44. Bryant HE, Schultz N, Thomas HD, Parker KM, Flower D, Lopez E, et al. Specific killing of BRCA2-deficient tumours with inhibitors of poly(ADP-ribose) polymerase. Nature 2005;434:913–7 [PubMed: 15829966]
45. Farmer H, McCabe N, Lord CJ, Tutt AN, Johnson DA, Richardson TB, et al. Targeting the DNA repair defect in BRCA mutant cells as a therapeutic strategy. Nature 2005;434:917–21 [PubMed: 15829967]
46. Tutt A, Robson M, Garber JE, Domchek SM, Audeh MW, Weitzel JN, et al. Oral poly(ADP-ribose) polymerase inhibitor olaparib in patients with BRCA1 or BRCA2 mutations and advanced breast cancer: a proof-of-concept trial. Lancet 2010;376:235–44 [PubMed: 20609467]
47. Bouwman P, Aly A, Escandell JM, Pieterse M, Bartkova J, van der Gulden H, et al. 53BP1 loss rescues BRCA1 deficiency and is associated with triple-negative and BRCA-mutated breast cancers. Nat Struct Mol Biol 2010;17:688–95 [PubMed: 20453858]
48. Bunting SF, Callen E, Wong N, Chen HT, Polato F, Gunn A, et al. 53BP1 inhibits homologous recombination in Brca1-deficient cells by blocking resection of DNA breaks. Cell 2010;141:243–54 [PubMed: 20362325]

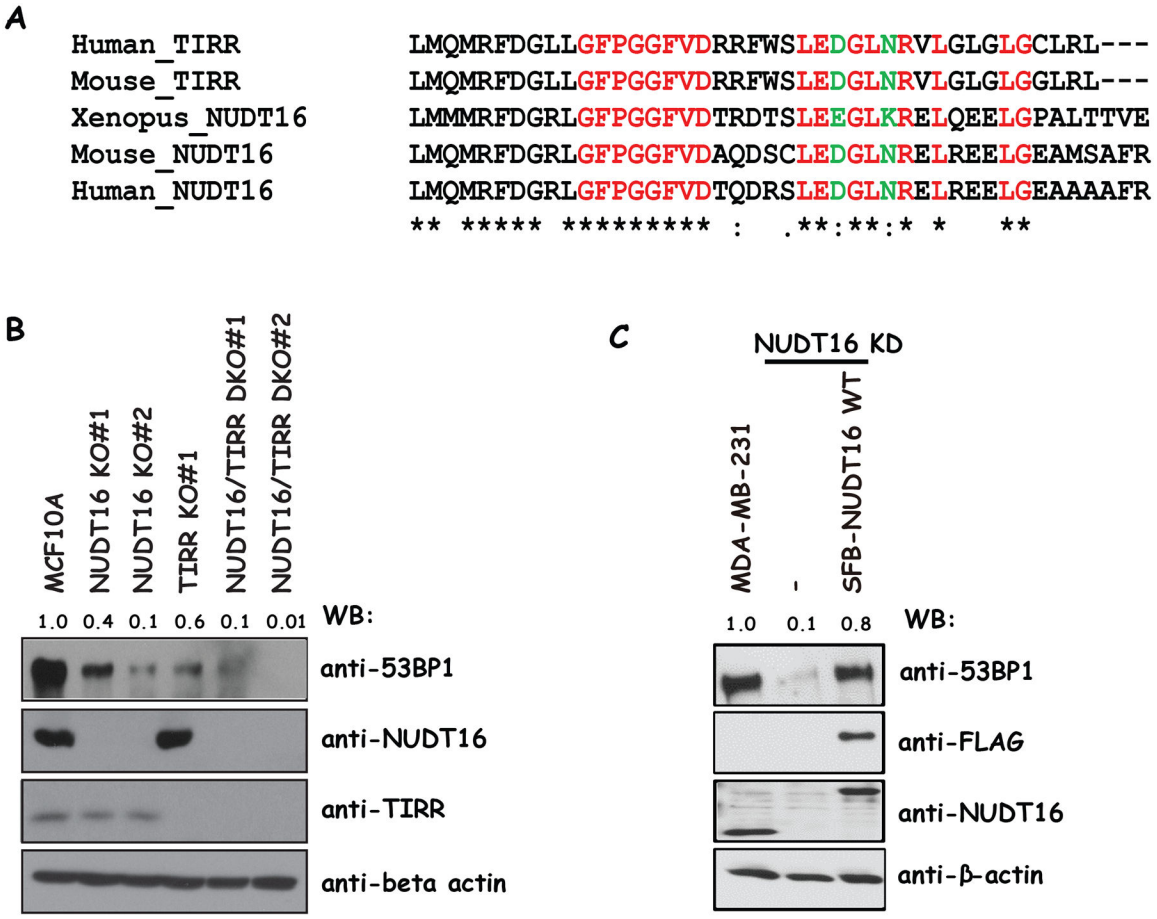

Figure 1. NUDT16 regulates 53BP1 stability.

A, Sequence alignment of the Nudix motif on TIRR and NUDT16 in different species. The conserved Nudix motif residues are highlighted in red. **B**, MCF10A and MCF10A-derived NUDT16 knockout (KO), TIRR KO and NUDT16/TIRR double KO cells were lysed with NTEN buffer and immunoblotted with the indicated antibodies. **C**, MDA-MB-231 cells were reconstituted with wild-type NUDT16. Then MDA-MB-231 and the reconstituted cells were infected with NUDT16 sgRNAs, and cells were lysed with NTEN buffer and immunoblotted with indicated antibodies.

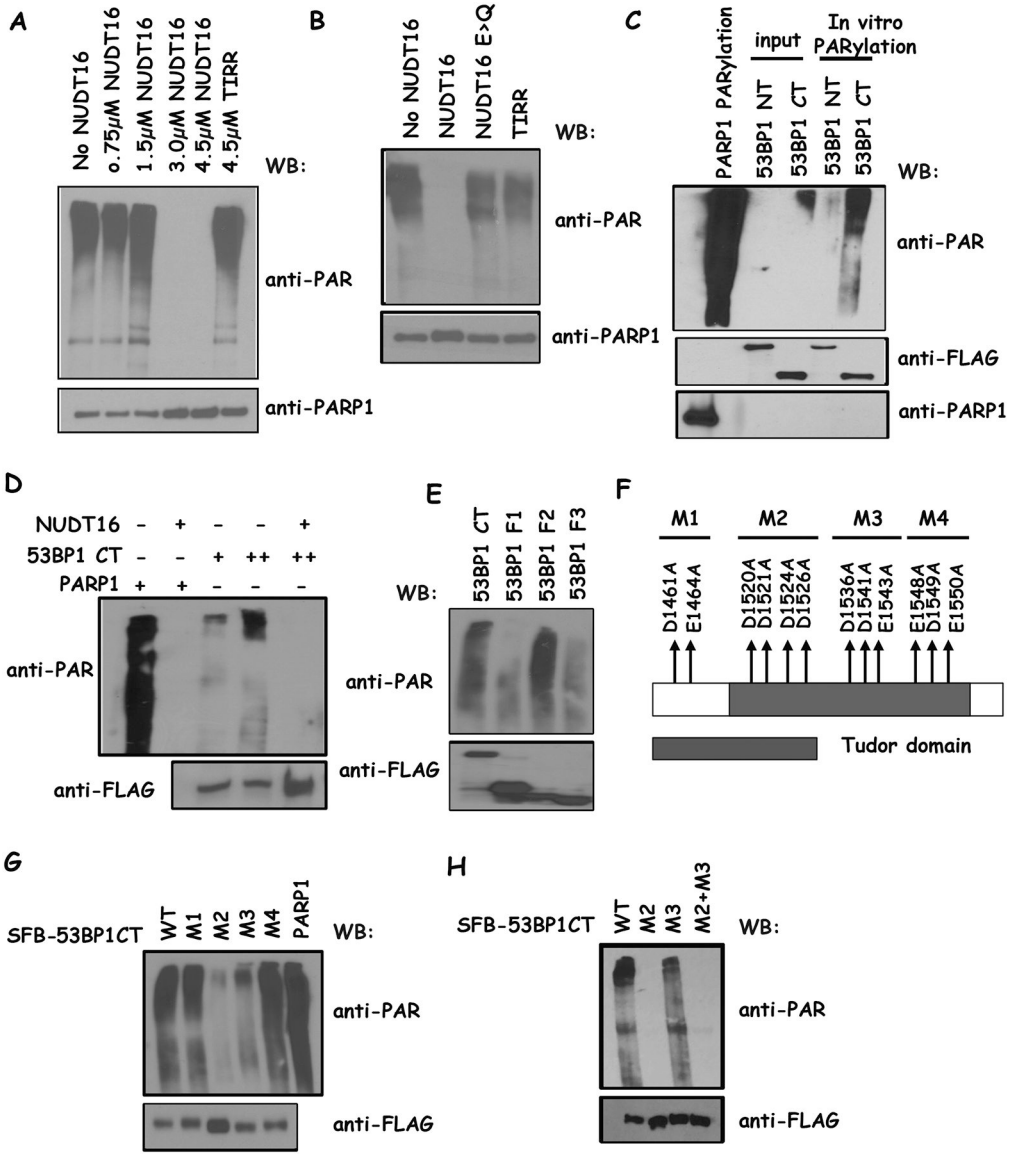

Figure 2. NUDT16 removes 53BP1 ADP-ribosylation.

A, *In vitro* PARylation assays were performed in a reaction mix consisting of different doses of bacterially expressed NUDT16 or TIRR proteins, PARP1 enzyme, 1xreaction buffer, 20μM NAD+, and 1xactive DNA for 30 minutes at room temperature (RT). The samples were immunoblotted with the indicated antibodies. **B**, *In vitro* PARylation assays were performed as described in (A) using bacterially expressed wild-type NUDT16 (3μM) or NUDT16 E>Q mutant proteins (3μM). Note: NUDT16E>Q mutant = E76QE79QE80Q. **C**, HEK293T cells were transfected with plasmids encoding SFB-tagged 53BP1 N terminus (NT, 1–1042aa) and 53BP1 C terminus (CT, 1043–1972aa). Cells were lysed with NTEN buffer on ice for 30 minutes. Clear cell lysates were incubated with streptavidin beads at 4°C for 3 hours. Then the beads were eluted with 2mg/ml biotin in NTEN buffer at 4°C for 2 hours. *In vitro* PARylation assays were performed in a reaction mix consisting of the eluates, 1xreaction buffer, 20μM NAD+, and 1xactive DNA for 30 minutes at RT. PARP1 enzyme

served as a positive control in a reaction mix without eluates. The samples were then immunoblotted with the indicated antibodies. **D**, The experiment was performed as described in (**C**). *In vitro* PARylation assays were performed with bacterially expressed wild-type NUDT16 (3μM) in a dose-dependent manner. **E**, The experiment was performed as described in (**C**). Note: 53BP1 F1=1354–1454aa; 53BP1 F2=1455–1557aa; 53BP1 F3=1558–1563aa; **F**, Schematic diagram of mutation sites on 53BP1. **G and H**, Identification of ADP-ribosylation sites on 53BP1. The experiment was performed as described in (**C**).

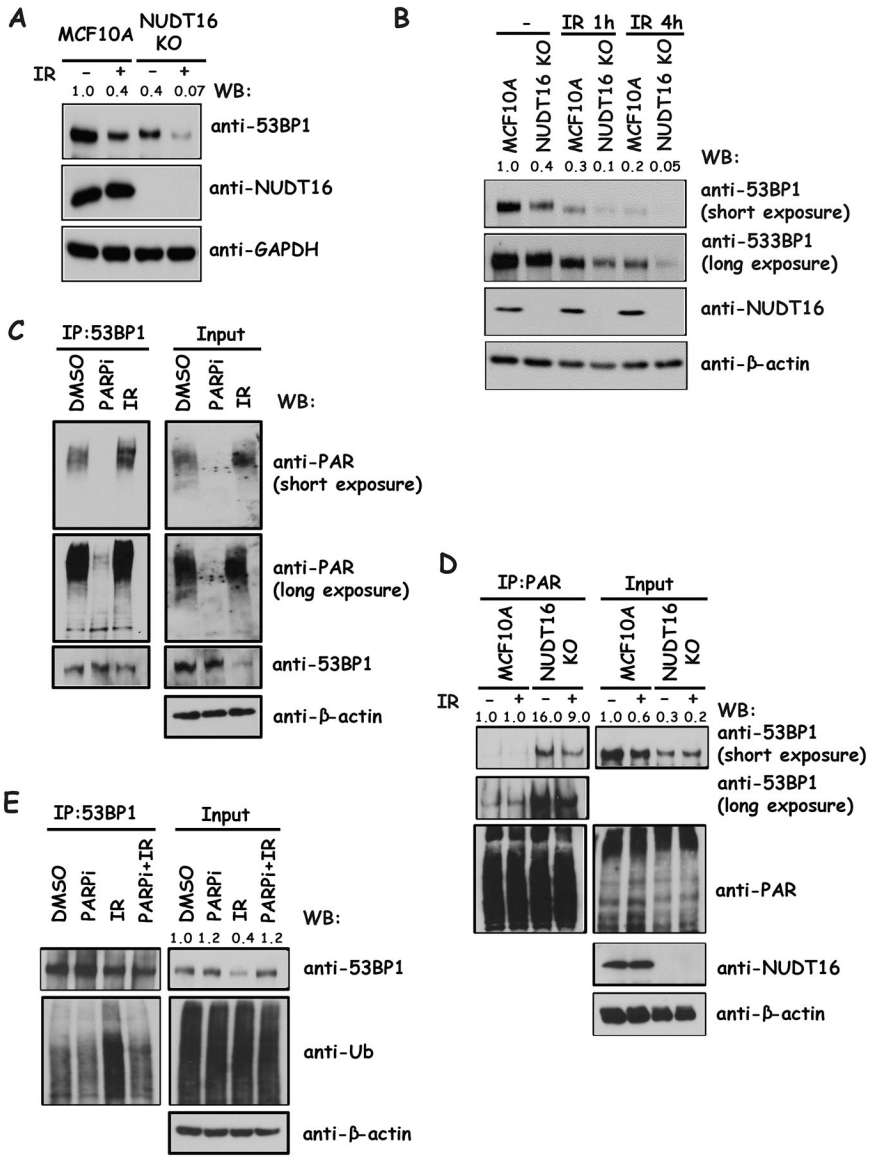

Figure 3. DNA damage-induced 53BP1 ADP-ribosylation leads to ubiquitination and degradation.

A, MCF10A and MCF10A derived NUDT16 KO cells were treated with or without IR (20 Gy) for 1 hour. Cells were lysed with NTEN buffer and immunoblotted with the indicated antibodies. **B**, MCF10A and MCF10A derived NUDT16 KO cells were treated with or without IR (20 Gy). Cells were lysed with NTEN buffer at indicated time points and immunoblotted with the indicated antibodies. **C**, MCF10A cells were mock treated (DMSO) or treated with a PARPi (10 μM olaparib) or IR (20 Gy). Cells were lysed with NTEN buffer 30 minutes after IR and immunoprecipitated with 53BP1 antibody. Immunoprecipitates were blotted using antibodies as indicated. **D**, MCF10A and NUDT16 KO cells were mock treated and IR (20 Gy). Cells were lysed with NTEN buffer 30 minutes after IR and immunoprecipitated with PAR antibody. Immunoprecipitates were blotted using antibodies as indicated. **E**, MCF10A cells were mock treated (DMSO) or treated with PARPi (20μM olaparib), IR (20 Gy) and PARPi (20μM olaparib)/IR (20 Gy). Cells were lysed with NTEN

buffer 30 minutes after IR and immunoprecipitated with 53BP1 antibody. Immunoprecipitates were blotted using antibodies as indicated.

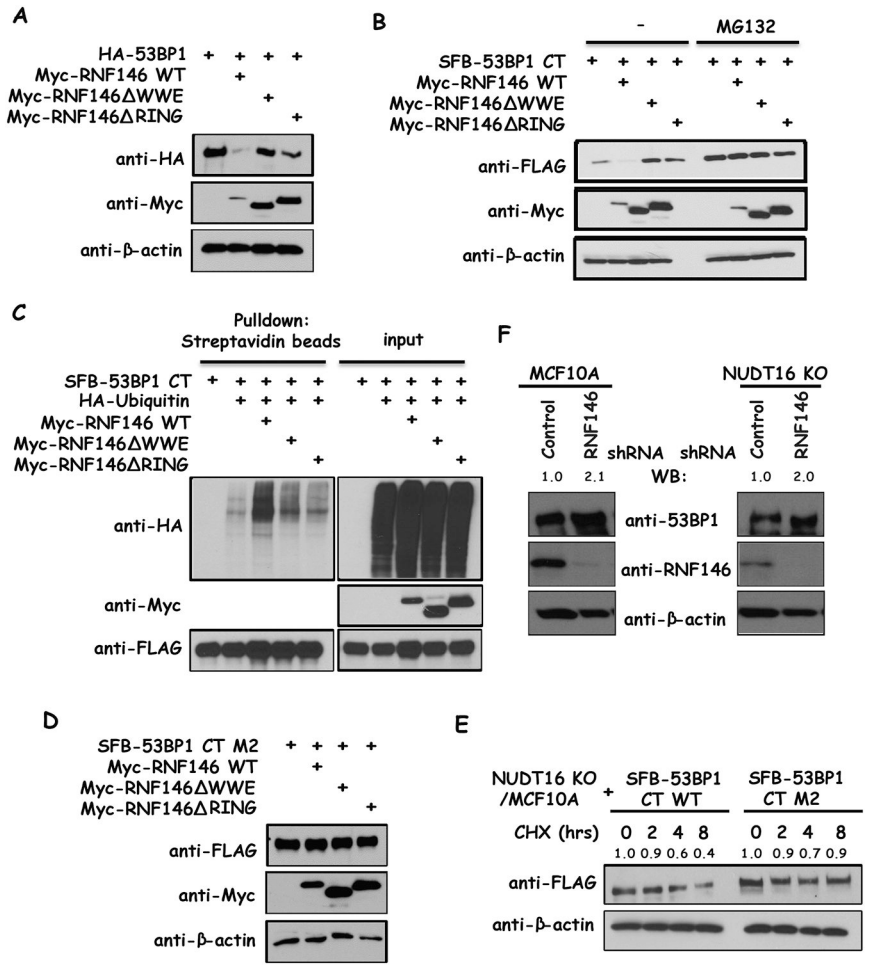

Figure 4. The E3 ligase RNF146 is required for ADP-ribosylation-dependent ubiquitination and degradation of 53BP1.

A-B, HEK293T cells were transfected with constructs encoding HA-53BP1 or SFB-53BP1 CT together with vector alone or constructs encoding Myc-tagged wild-type RNF146, the RNF146-ΔWWE mutant, or the RNF146-ΔRING mutant. At 24 hours after transfection, cells were treated with the proteasome inhibitor 20μM MG132 for 2 hours. Cell were lysed with NTEN buffer and examined by Western blotting using the indicated antibodies. **C**, 293T cells were transfected with constructs encoding HA-tagged ubiquitin, SFB-tagged 53BP1 CT, and Myc-tagged wild-type RNF146, the ΔWWE mutant of RNF146, or the ΔRING mutant of RNF146. At 24 hours after transfection, cells were treated with the proteasome inhibitor 20μM MG132 for 2 hours. Cells were lysed with NTEN buffer and analyzed by immunoprecipitation/Western blotting using the indicated antibodies. **D**, HEK293T cells were transfected with constructs encoding the M2 mutant of FB-53BP1 CT together with vector alone, or with constructs encoding Myc-tagged wild-type RNF146, the RNF146-ΔWWE mutant, or the RNF146-ΔRING mutant. Cells were lysed with NTEN buffer and examined by Western blotting using the indicated antibodies. **E**, MCF10A derived NUDT16 KO cells were reconstituted with wild-type or M2 mutant of SFB-53BP1 CT. After treatment with cycloheximide (CHX, 10μg/ml), cells were harvested at the indicated times and immediately lysed with 2xLaemmli buffer. The lysates were

immunoblotted with indicated antibodies. **F**, RNF146 knockdown cells and control MCF10 and NUDT16 KO/MCF10A cells were lysed with NTEN buffer and examined by Western blotting.

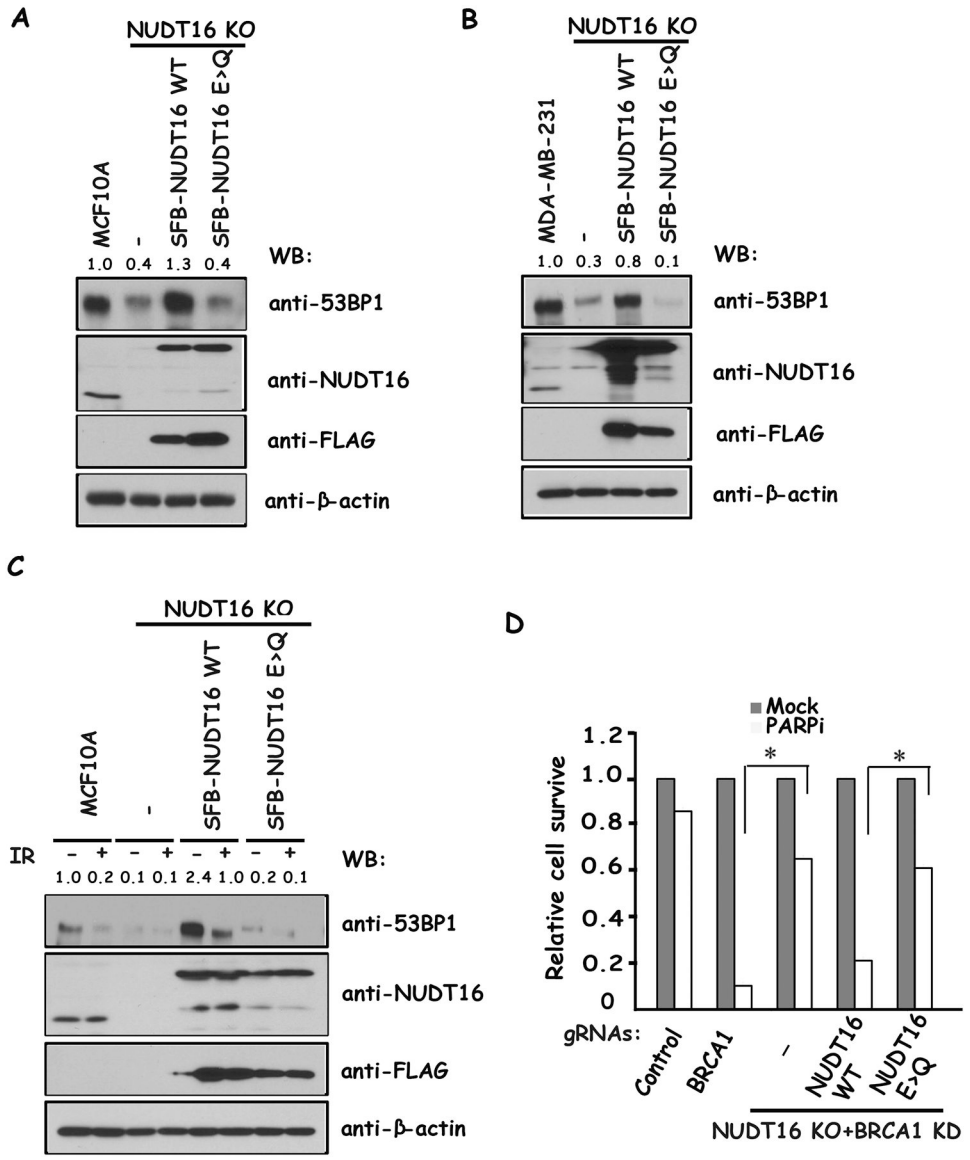

Figure 5. The catalytic activity of NUDT16 determines 53BP1 protein stability.

A, MCF10A and its derived NUDT16 KO cells were reconstituted with wild-type or the E>Q mutant of SFB-NUDT16. Cell were lysed with NTEN buffer and immunoblotted with the indicated antibodies. **B**, MDA-MB-231 and its derived NUDT16 KO cells were reconstituted with wild-type or the E>Q mutant of SFB-NUDT16. Cell were lysed with NTEN buffer and immunoblotted with the indicated antibodies. **C**, MCF10A and its derived NUDT16 KO cells were reconstituted with wild-type or the E>Q mutant of SFB-NUDT16. Cell were lysed with NTEN buffer 1 hour after IR, and immunoblotted with the indicated antibodies. **D**, MCF10A derived NUDT16 KO cells were reconstituted with wild-type or the E>Q mutant of SFB-NUDT16. These cells were infected with indicated gRNAs and treated with 1μm PARPi (olaparib). Colony formation was quantified relative to colonies formed in untreated cells. Data are represented as the mean ±S.E. (triplicate). *, $p<0.05$.

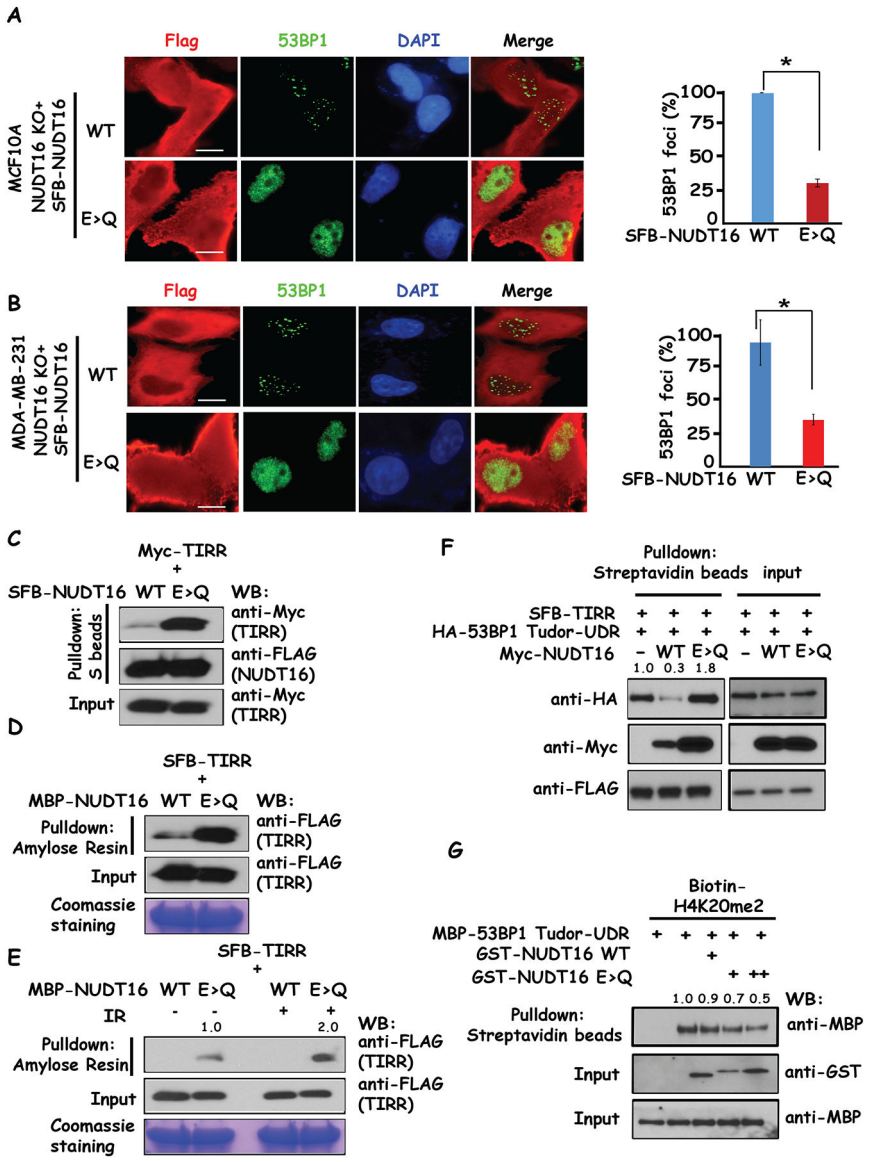

Figure 6. The catalytic activity of NUDT16 is critical for 53BP1 localization at DSBs.

A-B, MCF10A or MDA-MB-231 derived NUDT16 knockout cells were transfected with plasmids encoding wild-type or E>Q mutant of SFB-tagged NUDT16 followed by IR. Four hours later cells were fixed and immunostained with anti-FLAG and anti-53BP1. 53BP1 foci in these cells were quantified (at least 400 cells were counted for each experiment; three independent experiments). Data are represented as the mean ±S.E. *, $p<0.05$. Scale bar represents 20μm. **C**, HEK293T cells were transfected with plasmids encoding Myc-tagged TIRR together with the plasmid encoding wild-type or E>Q mutant of SFB-tagged NUDT16. Cells were lysed with NTEN buffer and immunoprecipitation reactions were conducted using S protein beads and then subjected to Western blotting using the indicated antibodies. **D**, Beads coated with bacterially expressed MBP-fused NUDT16 wild-type and E>Q mutant were incubated with cell lysates containing exogenously expressed SFB-tagged TIRR. Immunoblotting experiments were carried out using the indicated antibodies. **E**,

Beads coated with bacterially expressed MBP-fused NUDT16 wild-type or E>Q mutant were incubated with cell lysates containing exogenously expressed SFB-tagged TIRR treated with or without IR (20 Gy) for 1 hour. Immunoblotting experiments were carried out using the indicated antibodies. **F**, HEK293T cells were transfected with plasmids encoding SFB-tagged TIRR, HA-tagged 53BP1 Tudor-UDR together with the plasmid encoding wild-type or E>Q mutant of Myc-tagged NUDT16. Cells were lysed with NTEN buffer and immunoprecipitation reactions were conducted using streptavidin beads and then subjected to Western blotting using the indicated antibodies. **G**, Biotinylated histone H4K20me2 was incubated with bacterial expressed and purified MBP-53BP1 Tudor-UDR and GST-NUDT16 wild-type and E>Q mutant. Then streptavidin beads were added to the reaction and incubated. Beads were washed and boiled, and then subjected to Western blotting using the indicated antibodies.

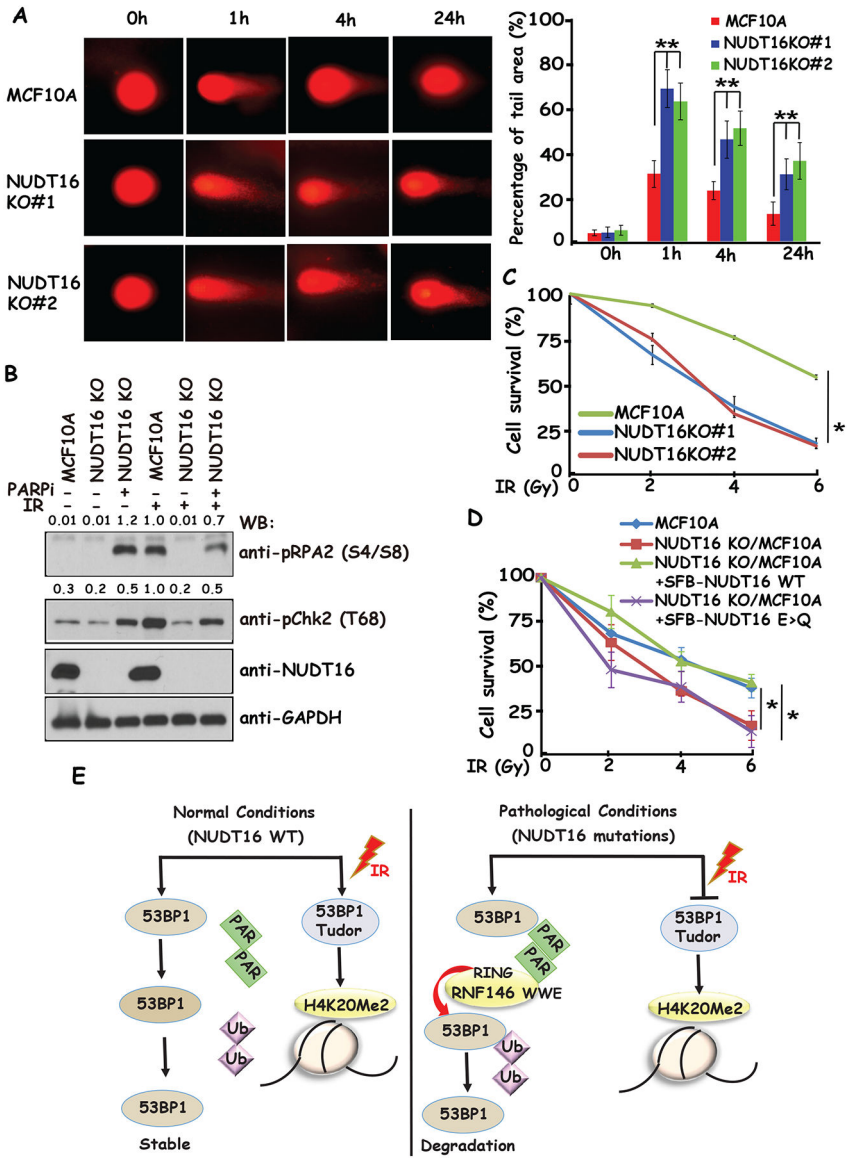

Figure 7. NUDT16 participates in the DNA damage response.

A, Loss of NUDT16 caused accumulation of DSBs as determined by a Comet assay performed as described in Materials and Methods. The comet tail area, expressed as a percentage of the entire comet, reflects the unrepaired DNA damage. Signal intensities were quantified, and a mean value for each time point was calculated from three independent experiments (right panel). At least 50 comets with tails were analyzed for each experiment. Data are shown as the mean ±S.E. *, $p<0.05$. **B**, MCF10A and its derived NUDT16 KO cells were treated with IR (20 Gy) or PARPi (20μM olaparib). Cells were lysed with NTEN buffer and analyzed by Western blotting using the indicated antibodies. **C**, MCF10A derived NUDT16 KO cells were mock-treated or treated with IR in a dose-dependent manner. Cell survival was measured by clonogenic assay as described in Materials and Methods. *, $p<0.05$. **D**, MCF10A derived NUDT16 KO cells were reconstituted with wild-type NUDT16 or the E>Q mutant of SFB-NUDT16. These cells were mock-treated or treated with IR in a

dose-dependent manner. Cell survival was measured by a clonogenic assay, as described in Materials and Methods. *, $p<0.05$. **E**, A working model representing the regulation of 53BP1 by NUDT16. Please see details in the Discussion.